Proc. Radiochim. Acta **1**, 123–126 (2011) / **DOI** 10.1524/rcpr.2011.0022

Cross sections of ^{7}Be, ^{22}Na and ^{24}Na for geochemical and cosmochemical important elements by monoenergetic 287 and 370 MeV neutrons

By K. Ninomiya[1,2,*], T. Omoto[1], R. Nakagaki[1], N. Takahashi[1], A. Shinohara[1], S. Sekimoto[3], T. Utsunomiya[3], H. Yashima[3], S. Shibata[3], T. Shima[4], N. Kinoshita[5], H. Matsumura[5], M. Hagiwara[5], Y. Iwamoto[2], D. Satoh[2], M. W. Caffee[6], K. C. Welten[7], M. Imamura[8] and K. Nishiizumi[7]

[1] Graduate School of Science, Osaka University, Toyonaka, Osaka, 560-0043, Japan
[2] Japan Atomic Energy Agency, Tokai, Naka, Ibaraki, 319-1195, Japan
[3] Research Reactor Institute, Kyoto University, Kumatori, Osaka, 590-0494, Japan
[4] Research Center for Nuclear Physics, Osaka University, Suita, Osaka, 567-0047, Japan
[5] High Energy Accelerator Research Organization, Tsukuba, Ibaraki, 305-0801, Japan
[6] Department of Physics, Purdue University, West Lafayette, IN 47907, USA
[7] Space Sciences Laboratory, University of California, Berkeley, CA 94720-7450, USA
[8] National Museum of Japanese History, Sakura, Chiba, 285-8502, Japan

(Received December 16, 2009; accepted in final form December 20, 2010)

Cross section / Neutron induced reaction / High energy neutron / Monoenergetic neutron / Short lived nuclide

Summary. Cross sections of ^{7}Be, ^{22}Na and ^{24}Na for geochemically and cosmochemically important elements were measured at incident neutron energies of 287 and 370 MeV. The cross sections were measured in target exposed to high-energy monoenergetic neutrons at the Research Center for Nuclear Physics (RCNP), Osaka University.

1. Introduction

Cross section measurements are a routine necessity for addressing many problems in nuclear structure. They are also the key to understanding numerous processes in geochemistry and cosmochemistry. For example, the detection of long-lived and stable nuclides produced by cosmic rays in meteorite, lunar rock and planetary material is essential for cosmic-ray exposure age determinations. These chronologies, in turn, inform us about the history of solar system materials and terrestrial landforms. Cosmic rays are comprised primarily of protons, however these protons are responsible for only a small fraction of the cosmogenic nuclide production, whether it is a meteoroid or a planetary atmosphere. It is the large cascade of secondary neutrons that interacting with the bulk of the target material that dominates most production pathways. Lacking measured cross sections, many neutron cross sections are estimated by using a proton cross section or calculated using theoretical models. These estimates, in many instances, have been found to be at variance with experimental data [1]. Unfortunately, few cross section measurements in the energy region > 20 MeV have been undertaken because of the difficulty in obtaining monoenergetic neutrons.

In recent years, some high energy monoenergetic neutron induced cross sections were reported. The neutron-induced cross section values up to 150 MeV of short lived nuclides were determined for Ti, Fe, Ni [2], Co [3], Cu [3, 4] and light elements [5, 6].

In this paper, we report a method using high energy monoenergetic neutrons at the Research Center for Nuclear Physics (RCNP), Osaka University. Production cross sections of ^{7}Be, ^{22}Na and ^{24}Na by monoenergetic 287 and 370 MeV neutron bombardment on C, N, O, Mg, Al, Si, K, Ca, Fe and Ni are also reported.

2. Experimental

To obtain monoenergetic neutron spectrum, we applied a recently developed technique [4] that allows as to eliminate the effects of unwanted low-energy neutrons. All proton irradiations were performed at N0 beam line in RCNP. The high energy neutrons were produced *via* the reaction of ^{7}Li $(p, n)^{7}$Be. The neutron production target was 11 mm thick enriched ^{7}Li metal (99.97%). The neutron energy spectra were measured using time-of-flight (TOF) at various angles ranging from 0° to 30° relative to the primary proton beam with 10–90 nA incident protons to determine the optimum condition for obtaining a monoenergetic neutron spectrum. These measurements indicate that monoenergetic neutron fluences were obtained for both the 0° and 30° irradiations. To determine the monoenergetic neutron cross sections for 287 and 370 MeV neutrons, irradiations of a day were performed using 300 and 392 MeV protons. The beam current was 1 μA.

*Author for correspondence
(E-mail: ninomiya.kazuhiko@jaea.go.jp).

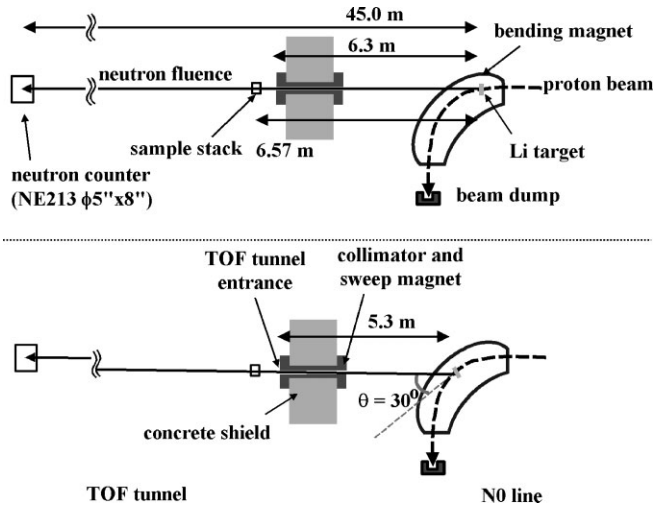

Fig. 1. Schematic view of neutron irradiation experiment at the N0 beam line and the TOF tunnel at RCNP for the 392 MeV primary proton beam from Ring-Cyclotron (upper: 0° irradiation, lower: 30° irradiation).

2.1 Neutron TOF measurement

Fig. 1 shows a schematic view of the experiment. The neutron production area (N0 line) is separated from the TOF tunnel by a 150 cm concrete shield and an iron collimator. The collimator is 12 cm high and 10 cm wide. Charged particles are stopped in the collimator, hence removed from the neutron flight path, by a bending magnet placed within the collimator. The neutron TOF measurements were performed at various angles relative to the incident proton direction by changing the position of Li target and the collimator. The start signal was taken from the timing signal from the accelerator. A NE213 organic liquid scintillation counter (20 cm diameter and 12.7 cm thick) was used as the stop detector for these measurements. Its location was 10.9 m from the TOF tunnel entrance for the 300 MeV experiment and 38.7 m for the 392 MeV experiment. Fig. 2 shows the neutron energy spectra for the 392 MeV proton beam. The intensity of the high-energy neutron component produced by the ^{7}Li(p, n) reaction decrease with increasing angles from 0° to 30°. As shown in previous work [4], the 0° neutron energy spectrum consists of a high-energy monoenergetic peak and a continuous low-energy component. The larger

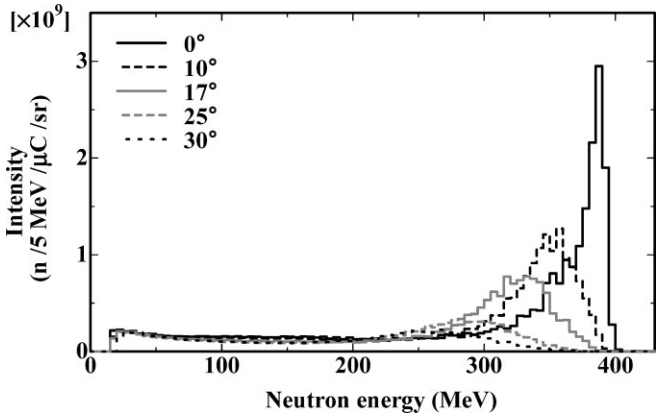

Fig. 2. Neutron energy spectra measured by the TOF method for 0°, 10°, 17°, 25° and 30° from the 392 MeV primary proton beam.

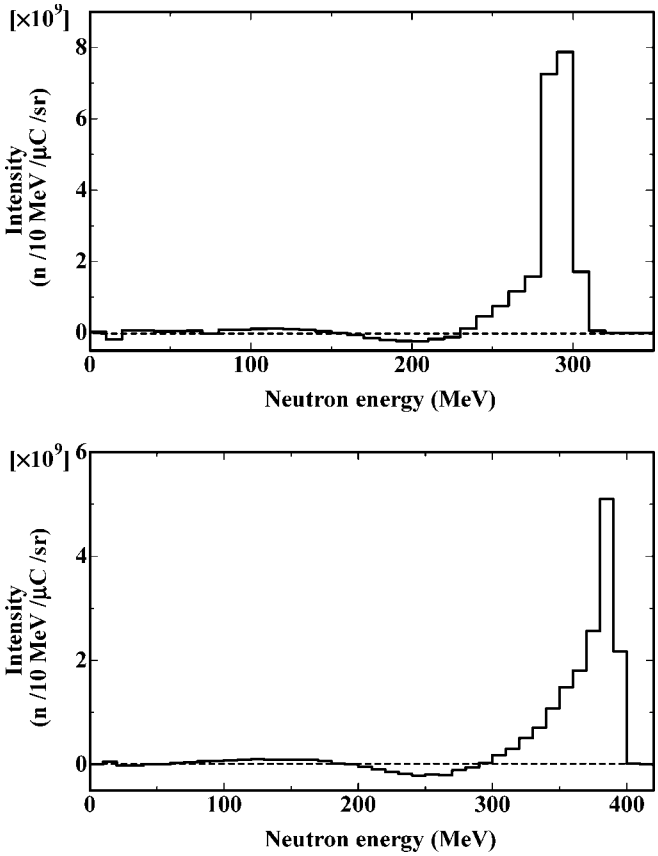

Fig. 3. Quasi-monoenergetic neutron spectra obtained by subtracting the 30° spectra multiplied by a correction factor from the 0° spectra (upper: 300 MeV primary proton beam, lower: 392 MeV primary proton beam).

angle spectrum consists only of the continuous low-energy component. We obtained the monoenergetic neutron spectra by subtracting the neutron spectra at larger angles from the 0° spectra, effectively eliminating the low-energy components. Test runs were performed for smaller angles (10° and 17°). Using these spectra for the subtraction resulted in negative neutron intensities at some energies. We found that the monoenergetic neutron spectra with the smallest low-energy component were obtained by subtracting 30° spectra from 0° spectra both for 300 and 392 MeV irradiations. The monoenergetic neutron spectra are shown in Fig. 3. The centroid of the neutron energy spectra occur at 287 ± 10 MeV and 370 ± 13 MeV for the 300 and the 392 MeV incident proton beams, respectively. The energy uncertainties of neutron fluences were determined from half maximum neutron intensities in the monoenergetic neutron spectra.

2.2 Cross-section measurements of monoenergetic neutron induced reactions for 287 and 370 MeV

Four equivalent stacks containing geochemical and cosmochemical important elements such as C, N, O, Mg, Al, Si, K, Ca, Fe and Ni (see Table 1 for detail) were prepared. Each sample stack was 10 cm high and 8 cm wide. We used these samples for four irradiation experiments; 0° and 30° irradiations both for 300 and 392 MeV primary proton beams. The sample stacks were located just behind from the TOF tunnel entrance (see Fig. 1): 70 cm for the 300 MeV and

Table 1. List of neutron irradiation samples. No enriched isotopic samples were used in this experiment. Each sample stack was separated with the following four parts; (A) Al, SiO_2, Fe, Ni, (B) Si, $CaCO_3$, (C) Mg, Cu, Nb, Au and (D) C, Si_3N_4, KNO_3. The sizes of (A) and (B) were 5×5 cm and (C) and (D) were 3×5 cm, respectively. The total size of the stack was 10 cm high and 8 cm wide. Since the production rates of ^{7}Be, ^{22}Na and ^{24}Na from Cu, Nb and Au samples are small, in this paper, we discuss the results from other samples (C, Mg, Al, Si SiO_2, Si_3N_4, KNO_3, $CaCO_3$, Fe, Ni) shown in this table.

Sample	Size (cm)	Typical weight (g)
C (plate)	3×5	5.2
Mg (plate)	3×3	8.4
Al (plate)	5×5	7.0
Si (plate)	5×5	37.8
Si_3N_4 (powder)[a]	3×5	48.7
SiO_2 (plate)	5×5	30.9
KNO_3 (powder)[a]	3×5	73.4
$CaCO_3$ (powder)[a]	5×5	98.7
Fe (plate)	5×5	63.5
Ni (plate)	5×5	72.1

a: Powder samples packed in plastic boxes.

27 cm for 392 MeV irradiations. The monoenergetic neutron fluxes at the sample position were estimated to be 4.27×10^4 /μC/cm^2 and 3.64×10^4 /μC/cm^2 for the 287 and the 370 MeV neutrons, respectively from neutron TOF measurement as shown in Sect. 2.1. The total number of incident neutrons for each experiment was estimated as 3.92 x 10^9 /cm^2 for 287 MeV and 3.45 x 10^9 /cm^2 for 370 MeV.

The production rates of ^{7}Be ($T_{1/2} = 53.12$ d, $E_\gamma = 478$ keV), ^{22}Na ($T_{1/2} = 2.604$ y, $E_\gamma = 1275$ keV) and ^{24}Na ($T_{1/2} = 14.95$ h, $E_\gamma = 1369, 2754$ keV) were measured using high purity germanium detectors. By subtracting the production rate in 30° irradiation multiplied by a correction factor from that in 0°, the production rates for monoenegetic 287 and 370 MeV neutron induced reactions were obtained. The neutron cross sections were calculated by combining the production rates with the estimated neutron fluxes.

Since the cross sections for most radionuclides are low, we compensated for the low neutron intensity by using large sample quantity. This has the side-effect of producing self-shielding in the detector. Therefore, the detection efficiencies of the germanium detectors for each gamma-ray energy and sample were determined from Monte Carlo simulation (Electron Gamma Shower-5: EGS-5 [7]). The parameters for EGS-5 were adjusted to reproduce the experimental detection efficiencies obtained from point source measurements at more than five different positions for each detector.

3. Results and discussion

The neutron-induced cross sections measured in this work are summarized in Table 2. The cross sections of ^{7}Be for N and O were determined after removing the contributions from Si$(n, x)^7$Be reactions in Si_3N_4 and SiO_2. The same corrections were done for $CaCO_3$ and KNO_3 to determine the cross-sections of Ca$(n, x)^7$Be and K$(n, x)^7$Be. The stated uncertainty includes statistical measurement errors and systematic errors arising from the correction of the monoenergetic neutron spectra (10%). We also estimate the systematic errors from gamma-ray detection efficiency (10%), neutron detection efficiency in NE213 detector (15%) and primary beam current monitoring (5%). Our neutron-induced cross sections obtained from subtraction between two irradiations are compared with the recent proton induced cross sections in the similar incident energy regions: 250–300 MeV for

Table 2. Neutron induced cross sections (mb) at 287 and 370 MeV. Data include systematic errors, *i.e.*, contribution of low energy neutrons (10%), gamma-ray detection efficiency (10%), neutron detection efficiency (15%) and beam monitoring (5%) as well as statistic errors. For some nuclear reactions, positive and negative uncertainties were obtained because only an upper limit for the production rate in the 30° irradiation was determined from the gamma-ray measurement.

Reaction	Cross section at 287 MeV (mb)	Cross section at 370 MeV (mb)
C$(n, x)^7$Be	4.7 ± 2.3	8.0 ± 3.3
N$(n, x)^7$Be	5.3 ± 2.2	
O$(n, x)^7$Be	3.4 ± 1.4	5.3 ± 2.0
Mg$(n, x)^7$Be	$2.3^{+1.2}_{-1.5}$	4.3 ± 1.5
Mg$(n, x)^{22}$Na	17.3 ± 5.9	23.5 ± 7.3
Mg$(n, x)^{24}$Na	12.0 ± 3.9	7.2 ± 2.5
Al$(n, x)^7$Be	$1.2^{+1.1}_{-1.2}$	$3.7^{+2.4}_{-3.7}$
Al$(n, x)^{22}$Na	10.4 ± 4.2	11.4 ± 5.7
Al$(n, x)^{24}$Na	14.5 ± 4.7	17.8 ± 5.7
Si$(n, x)^7$Be	1.0 ± 0.5	3.3 ± 1.2
Si$(n, x)^{22}$Na	8.0 ± 2.6	15.2 ± 4.9
Si$(n, x)^{24}$Na	6.1 ± 2.0	7.5 ± 2.4
K$(n, x)^7$Be	1.8 ± 3.9	
K$(n, x)^{24}$Na	1.2 ± 0.4	
Ca$(n, x)^7$Be	1.5 ± 3.4	
Ca$(n, x)^{22}$Na		2.0 ± 1.3
Ca$(n, x)^{24}$Na	1.0 ± 0.3	1.3 ± 0.4
Fe$(n, x)^7$Be		$1.7^{+1.0}_{-1.4}$
Fe$(n, x)^{24}$Na		0.14 ± 0.06
Ni$(n, x)^7$Be		$2.3^{+1.5}_{-2.3}$
Ni$(n, x)^{24}$Na	0.01 ± 0.02	0.11 ± 0.06

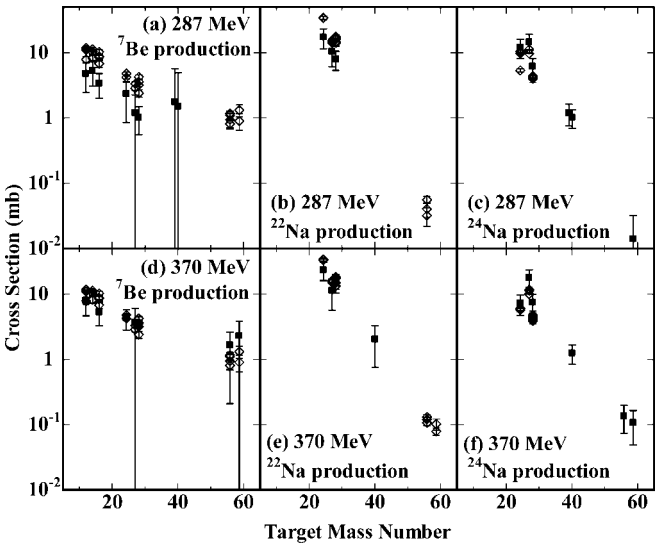

Fig. 4. Comparison of cross sections between proton- and neutron-induced reactions against the masses of target elements: (**a**) ^{7}Be production at 287 MeV, (**b**) ^{22}Na production at 287 MeV, (**c**) ^{24}Na production at 287 MeV, (**d**) ^{7}Be production at 370 MeV, (**e**) ^{22}Na production at 370 MeV and (**f**) ^{24}Na production at 370 MeV. The closed squares are neutron induced cross sections (this work) and the open diamonds are proton induced cross sections within a comparable energy region (250–300 MeV for 287 MeV neutron induced reactions and 350–400 MeV for 370 MeV neutron induced reactions) [8–13].

287 MeV neutron reactions and 350–400 MeV for 370 MeV neutron reactions (see Fig. 4) [8–13]. The cross section values for neutron induced reactions become smaller with increasing mass number. A target mass number dependence of the cross section is also observed in proton induced reactions. In general, the absolute cross section of the neutron induced reactions were different from proton induced reactions; the production rates of neutron deficient nuclides (^{7}Be and ^{22}Na) by protons were larger than these by neutrons and the opposite tendency was obtained in neutron rich nuclide (^{24}Na). A more detailed investigation of this observation would require cross sections for the different product nuclides.

In summary, we successfully obtained monoenergetic 287 and 370 MeV neutron fluences in RCNP, and determined the cross sections of ^{7}Be, ^{22}Na and ^{24}Na for geochemically and cosmochemically important elements (C, N, O, Mg, Al, Si, K, Ca, Fe and Ni). We are also planning to measure the cross sections of long-lived nuclides (*e.g.* ^{10}Be, ^{26}Al, ^{36}Cl and ^{53}Mn) for high energy monoenergetic neutron induced reactions (> 100 MeV) using AMS. These cross sections will contribute to our understanding of processes involving the interactions of cosmic rays with terrestrial and extraterrestrial materials.

Acknowledgment. The authors express their gratitude to the accelerator staff of RCNP for their generous support of this experiment (RCNP-E298). This study was partially supported by National Science Foundation (EAR-0345817).

References

1. Reedy, R. C., Arnold, J. R., Lal, D.: Cosmic-ray records in solar system matter. Ann. Rev. Nucl. Part. Sci. **33**, 505 (1983).
2. Sisterson, J. M., Chadwick, M. B.: Cross section measurements for neutron-induced reactions in Ti, Fe and Ni at several neutron energies ranging from 70.7 to 151.6 MeV. Nucl. Instrum. Methods B **245**, 371 (2006).
3. Kim, E. J., Nakamura, T., Uwamino, Y., Nakanishi, N., Imamaura, M., Nakao, N., Shibata, S., Tanaka, S.: Measurements of activation cross section on spallation reactions for ^{59}Co and ^{nat}Cu at incident neutron energies of 40 to 120 MeV. J. Nucl. Sci. Tech. **36**, 29 (1999).
4. Sisterson, J. M., Brooks, F. D., Buffler, A., Allie, M. S., Jones, D. T. L., Chadwick, M. B.: Cross-section measurements for neutron-induced reactions in copper at neutron energies of 70.7 and 110.8 MeV. Nucl. Instrum. Methods B **240**, 617 (2005).
5. Imamura, M., Nagai, H., Takabatake, M., Shibata, S., Kobayashi, K., Yoshida, K., Ohashi, H., Uwamino, Y., Nakamura, T.: Measurements of production cross sections of ^{14}C and ^{26}Al with high-energy neutrons up to $E_n = 38$ MeV by accelerator mass spectrometry. Nucl. Instrum. Methods B **52**, 595 (1990).
6. Sisterson, J. M.: Cross section measurements for neutron-induced reactions off C, Al, SiO_2, Si and Au producing relatively short-lived radionuclides at neutron energies between 70 and 160 MeV. Nucl. Instrum. Methods B **261**, 993 (2007).
7. Hirayama, H., Namito, Y., Bielajew, A. F., Wilderman, S. J., Nelson, W. R.: The EGS5 code system. SLAC-R 730 (2005).
8. Schiekel, Th., Sudbrock, F., Herpers, U., Gloris, M., Lange, H.-J., Leya, I., Michel, R., Dittrich-Hannen, B., Synal, H.-A., Suter, M., Kubik, P. W., Blann, M., Filges, D.: Nuclide production by proton-induced reactions on elements ($6 \leq Z \leq 29$) in the energy range from 200 MeV to 400 MeV. Nucl. Instrum. Methods B **114**, 91 (1996).
9. Sisterson, J. M., Kim, K., Beverding, A., Englert, P. A. J., Caffee, M., Jull, A. J. T., Donahue, D. J., McHargue, L., Castaneda, C., Vincent, J., Reedy, R. C.: Measurement of proton production cross sections of ^{10}Be and ^{26}Al from elements found in lunar rocks. Nucl. Instrum. Methods B **123**, 324 (1997).
10. Michel, R., Bodemann, R., Busemann, H., Daunke, R., Gloris, M., Lange, H.-J., Klug, B., Krins, A., Leya, I., Lüpke, M., Neumann, S., Reinhardt, H., Schnatz-Büttgen, M., Herpers, U., Schiekel, Th., Sudbrock, F., Holmqvist, B., Condé, H., Malmborg, P., Suter, M., Dittrich-Hannen, B., Kubik, P.-W., Synal, H.-A., Filges, D.: Cross sections for the production of residual nuclides by low- and medium-energy protons from the target elements C, N, O, Mg, Al, Si, Ca, Ti, V, Mn, Fe, Co, Ni, Cu, Sr, Y, Zr, Nb, Ba and Au. Nucl. Instrum. Methods B **129**, 153 (1997).
11. Faßbender, M., Scholten, B., Qaim, S. M.: Radiochemical studies of (p, ^{7}Be) reactions on biologically relevant elements in the proton energy range of 50 to 350 MeV. Radiochim. Acta. **81**, 1 (1998).
12. Faßbender, M., Shubin, Yu. N., Qaim, S. M.: Formation of activation products in interactions of medium energy protons with Na, Si, P, S, Cl, Ca and Fe. Radiochim. Acta. **84**, 59 (1999).
13. Morgan, G. L., Alrick, K. R., Saunders, A., Cverna, F. C., King, N. S. P., Merrill, F. E., Waters, L. S., Hanson, A. L., Greene, G. A., Liljestrand, R. P., Thompson, R. T., Henry, E. A.: Total cross sections for the production of ^{22}Na and ^{24}Na in proton-induced reactions on ^{27}Al from 0.40 to 22.4 GeV. Nucl. Instrum. Methods B **211**, 297 (2003).